ORGANIC
LETTERS

2007
Vol. 9, No. 6
1085−1088

Helical Growth of Semiconducting Columnar Dye Assemblies Based on Chiral Perylene Bisimides

**Volker Dehm,[†] Zhijian Chen,[†] Ute Baumeister,[‡] Paulette Prins,[§]
Laurens D. A. Siebbeles,[§] and Frank Würthner*,[†]**

Institut für Organische Chemie and Röntgen Research Center for Complex Material Systems, Universität Würzburg, Am Hubland, 97074 Würzburg, Germany, Institut für Physikalische Chemie, Martin-Luther-Universität Halle-Wittenberg, Mühlpforte 1, 06108 Halle, Germany, and Opto-electronic Materials Section, DelftChemTech, Delft University of Technology, NL-2629 JB Delft, The Netherlands

wuerthner@chemie.uni-wuerzburg.de

Received January 12, 2007

ABSTRACT

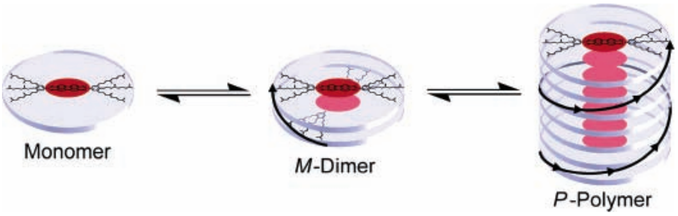

A perylene bisimide derivative bearing two phenyl substituents with chiral solubilizing alkyl chains at the imide N atoms has been synthesized, and its self-assembly properties in solution and condensed phase have been investigated. Temperature-dependent CD spectra revealed the coexistence of two different kinds of chiral aggregates, differing in size and handedness. The chiral side chains effect a higher order within the self-assemblies, resulting in an increased charge-carrier mobility in the columnar liquid crystalline mesophase.

Helical self-organization by noncovalent interactions is a widely observed feature of natural biomacromolecules that directs the formation of highly ordered structures, e.g., the spontaneous self-assembly of DNA into a double helix and of proteins and polysaccharides into α-helices. Inspired by the unique features of fascinating biological superstructures, numerous artificial assemblies have been developed in the past decades by utilizing noncovalent forces such as hydrogen bonding, metal ion coordination, and $\pi-\pi$ interaction.[1] Recently, several groups have initiated programs to engineer functional materials for electronic devices by proper control of the packing of π-conjugated molecules by such noncovalent interactions.[2−5] In particular, various examples of discotic molecules such as triphenylenes,[3] hexabenzocoronenes,[4] and phthalocyanines[5] have been reported to form π stacks with helical superstructures that exhibit increased charge-carrier mobilities as a result of the higher molecular order imparted by the helical stacking arrangement.

Although all of these above-mentioned molecules possess electron-rich aromatic cores that give rise to columnar π stacks with p-type semiconducting properties, we have

---

[†] Universität Würzburg.
[‡] Martin-Luther-Universität Halle-Wittenberg.
[§] Delft University of Technology.

(1) Cornelissen, J. J. L. M.; Rowan, A. E.; Nolte, R. J. M.; Sommerdijk, N. A. J. M. *Chem. Rev.* **2001**, *101*, 4039.

(2) (a) Percec, V.; Glodde, M.; Bera, T. K.; Miura, Y.; Shiyanovskaya, I.; Singer, K. D.; Balagurusamy, V. S. K.; Heiney, P. A.; Schnell, I.; Rapp, A.; Spiess, H.-W.; Hudson, S. D.; Duan, H. *Nature* **2002**, *417*, 384. (b) Hill, J. P.; Jin, W.; Kosaka, A.; Fukushima, T.; Ichihara, H.; Shimomura, T.; Ito, K.; Hashizume, T.; Ishii, N.; Aida, T. *Science* **2004**, *304*, 1481. (c) For a recent review, see: Schenning, A. P. H. J.; Meijer, E. W. *Chem. Commun.* **2005**, *3245*.

(3) Adam, D.; Schumacher, P.; Simmerer, J.; Häusling, L.; Siemensmeyer, K.; Etzbach, K. H.; Ringsdorf, H.; Harrer, D. *Nature* **1994**, *371*, 141.

(4) Wu, J.; Watson, M. D.; Zhang, L.; Wang, Z.; Müllen, K. *J. Am. Chem. Soc.* **2004**, *126*, 177.

(5) Engelkamp, H.; Middlebeek, S.; Nolte, R. J. M. *Science* **1999**, *284*, 785.

10.1021/ol0700963 CCC: $37.00

Scheme 1. Synthesis of the Chiral PBI **3**

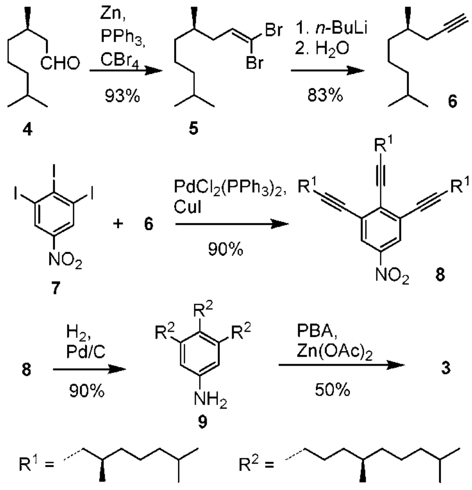

recently discovered that also the considerably elongated electron-poor π-electron system perylene bisimides (PBI), e.g., the derivatives **1** and **2**, preferentially stack in a columnar fashion due to rotational displacements of neighboring molecules.[6,7] However, owing to the achiral nature of these PBI building blocks, no chiral supramolecular ordering could be observed on a macroscopic level; rather, disordered hexagonal columnar mesophases were found.

In the absence of chiral units in these PBI molecules, both possible helical conformations (i.e., *M* and *P*) necessarily have equal intermolecular interaction energies; therefore, racemic mixtures of helical assemblies can be expected. However, by means of chiral side chains, the *M*/*P* chemical equilibrium can be biased, which affords a preferential helicity on the higher supramolecular level of organization.[8] Thus, we envisioned that PBI derivatives containing chiral side chains should afford nonracemic helical supramolecular structures.

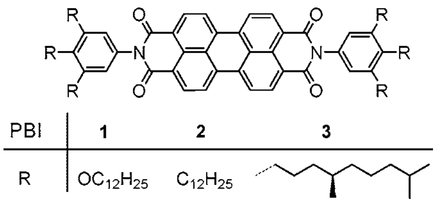

Here, we present a new chiral PBI derivative **3**, which indeed affords helical superstructures upon self-assembly. Much to our surprise, the self-assembly studies of this chiral building block in apolar aliphatic solutions revealed some striking aspects with regard to the development of chiral order upon columnar growth, and the condensed liquid crystalline (LC) phase of **3** showed an improved charge-carrier mobility.

The PBI derivative **3** with six appended chiral side chains was synthesized in five steps starting with the known aldehyde **4**[9] according to Scheme 1. The details of the synthesis are given in Supporting Information.

The self-assembly behavior of PBI dye **3** in solution was studied by UV/vis absorption spectroscopy in methylcyclohexane (MCH). As shown in Figure 1, at low concentrations an absorption band with a well-resolved vibrational fine structure between 400 and 530 nm was observed that can be attributed to the $S_0 \rightarrow S_1$ transition of the perylene bisimide monomer.

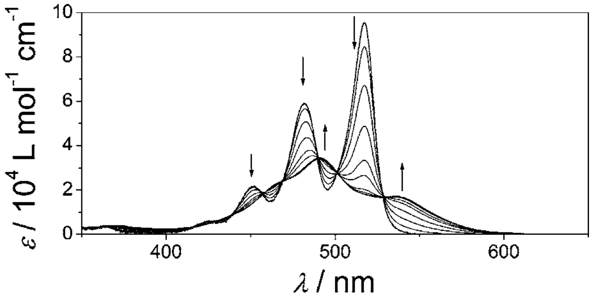

Figure 1. Concentration-dependent UV/vis absorption spectra of PBI **3** (10^{-6} to 2×10^{-3} M) in MCH at 25 °C. Arrows indicate changes upon increasing concentration.

The absorption maximum appeared at 517 nm, along with two higher vibronic transitions located at 482 and 451 nm. Upon increasing the concentration, the absorption coefficient dramatically decreased and a blue shift of the absorption maximum to 491 nm was observed. In addition, a second red-shifted absorption band of lower intensity at 536 nm evolved. Owing to the presence of well-defined isosbestic points at 469, 502, and 529 nm, we may be tempted to conclude that only two different kinds of absorbing species are in equilibrium. The observed spectral changes at higher concentrations can be attributed to excitonic coupling between closely $\pi-\pi$-stacked perylene bisimides with rotational displacements of about 55° between the neighboring dyes.[10] Temperature-dependent UV/vis spectra (Figure S1 in Supporting Information) reveal similar spectral features as observed in the concentration-dependent measurements. This suggests that the spectral changes originate from the same process, i.e., self-assembly of monomeric dyes into larger aggregates composed of $\pi-\pi$-stacked species.

By means of concentration- and temperature-dependent UV/vis spectroscopy for **3** in MCH (from 10 to 70 °C in intervals of 10 °C), we were able to determine the enthalpy

---

(6) Würthner, F.; Thalacker, C.; Diele, S.; Tschierske, C. *Chem.—Eur. J.* **2001**, *7*, 2245.

(7) Chen, Z.; Stepanenko, V.; Dehm, V.; Prins, P.; Siebbeles, L. D. A.; Seibt, J.; Marquetand, P.; Engel, V.; Würthner, F. *Chem.—Eur. J.* **2007**, *13*, 436.

(8) (a) Palmans, A. R. A.; Vekemans, J. A. J. M.; Havinga, E. E.; Meijer, E. W. *Angew. Chem., Int. Ed.* **1997**, *36*, 2648. (b) Brunsveld, L.; Zhang, H.; Glasbeek, M.; Vekemans, J. A. M. J.; Meijer, E. W. *J. Am. Chem. Soc.* **2000**, *122*, 6175. (c) van Herrikhuyzen, J.; Syamakumari, A.; Schenning, A. P. H. J.; Meijer, E. W. *J. Am. Chem. Soc.* **2004**, *126*, 10021. (d) Nakade, H.; Jordan, B. J.; Xu, H.; Han, G.; Srivastava, S.; Arvizo, R. R.; Cooke, G.; Rotello, V. M. *J. Am. Chem. Soc.* **2006**, *128*, 14929. (e) Pantos, G. D.; Pengo, P.; Sanders, J. K. M. *Angew. Chem., Int. Ed.* **2007**, *46*, 194.

(9) Dolby, L. J.; Debondo, M. *J. Org. Chem.* **1964**, *29*, 2306.

(10) Seibt, J.; Marquetand, P.; Engel, V.; Chen, Z.; Dehm, V.; Würthner, F. *Chem. Phys.* **2006**, *328*, 354.

and entropy values of $\Delta H° = -58.9 \pm 1.0$ kJ mol^{-1} and $\Delta S° = -107.9 \pm 0.1$ J mol^{-1} K^{-1} for this self-assembly process from the linear van't Hoff plot (Figure S2 in Supporting Information). In our recent work,[7] we have reported in detail on the calculation of average aggregation numbers *N* from UV/vis data of similar one-dimensional self-assemblies of PBI derivative **2** based on the isodesmic model (also referred to as the equal *K* model)[11] and confirmed these results by vapor pressure osmometry and DOSY NMR studies. By applying this method to the concentration- and temperature-dependent (from −10 to 90 °C) UV/vis spectral data of PBI dye **3**, we could estimate average aggregation numbers (*N*) for a 2×10^{-3} M solution of **3** in MCH at different temperatures. Thus, at −10, 40, and 90 °C, the *N* values of 55, 6, and 2, respectively, were obtained. A complete set of data are given in Table S2 in the Supporting Information.

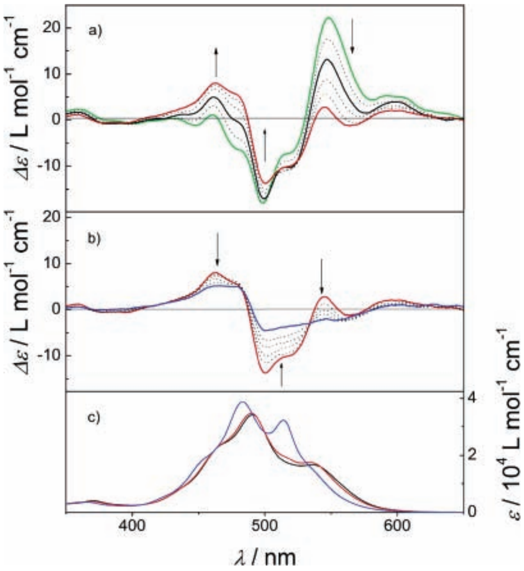

Figure 2. Temperature-dependent CD and UV/vis spectra of **3** (2×10^{-3} M) in MCH. (a) CD spectra from −10 to 40 °C (green line, −10 °C; black line, 10 °C; red line, 40 °C), in intervals of 10 °C. (b) CD spectra from 40 to 90 °C (red line, 40 °C; blue line, 90 °C), in intervals of 10 °C. Arrows indicate changes upon increasing temperature. (c) UV/vis spectra at 10, 40, and 90 °C (black, red, and blue line, respectively).

As can be seen in Figure 2c, the remarkable increase in aggregate size, i.e., higher *N* values, upon cooling the sample from 40 to 10 °C (*N* value increased from 6 to 34), does not affect the shape of the UV/vis absorption spectrum significantly. Thus, aggregates of different sizes, i.e., dimers, trimers, etc., cannot be discriminated by this method. Only at higher temperature, where the molar fraction of the monomer increases, is a notable change in the shape of absorption bands observed (blue line in Figure 2c).

Recent studies on self-assembly of chiral π-conjugated molecules have revealed that a deeper insight into aggregation processes can be gained by CD spectroscopy.[8,12] Thus, the impact of the molecular chiral side chains of **3** on the supramolecular order of its $\pi-\pi$-stacked aggregates was examined by temperature-dependent CD spectroscopy (Figure 2a,b). No CD signal could be observed for the PBI **3** monomer in dichloromethane (DCM) solution between 350 and 650 nm, whereas for the aggregates of **3** in concentrated MCH solution, a strong induced bisignate Cotton effect was observed at −10 °C with a positive maximum at 548 nm and a negative maximum at 498 nm (Figure 2a, green line).

Upon heating from −10 (green line) to 40 °C (red line), the Cotton effect at 548 nm completely vanished, whereas the one at 498 nm was diminished. On the other hand, a positive CD band emerged at 462 nm and a negative shoulder appeared at 512 nm. Further heating of the sample to 90 °C (Figure 2b, blue line) resulted in an overall decrease of the CD signal, but even at this high temperature, dimeric species prevail as the bisignate CD signal with a negative maximum at 500 nm and a positive maximum at 460 nm as well as the UV/vis spectra (Figure 2c) reveal. The aggregation process of **3** is fully reversible, as upon cooling the sample from 90 to −10 °C the initial CD spectrum is recovered.

On the basis of the *N* values given in Table S2 in the Supporting Information, one can relate the CD spectrum at 90 °C to PBI dimers, whereas the CD spectrum at −10 °C originates from extended species with average aggregation numbers greater than 50. At intermediate temperatures, complex CD spectra arise that lack defined isodichroic points. This observation does not comply with the earlier conclusion of a two-state equilibrium that was drawn based on well-defined isosbestic points observed in UV/vis spectra. According to CD spectroscopy, an equilibrium among at least three different species has to be considered to account for the observed temperature-dependent features in the CD spectra, as proposed in Figure 3.

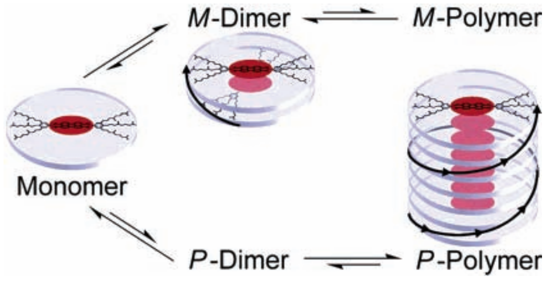

Figure 3. Proposed equilibrium of monomer and aggregated species of PBI **3** in solution. At low concentration and/or high temperature, dimers are formed that are preferentially of *M*-type helicity. Upon further growth into extended polymeric stacks, *P*-configured species are preferred.

The low-temperature CD spectra indicate the preferential formation of right-handed (*P*-configured) extended ag-

---

[11] Martin, R. B. *Chem. Rev.* **1996**, *96*, 3043.

[12] (a) Jonkheijm, P.; van der Schoot, P.; Schenning, A. P. H. J.; Meijer, E. W. *Science* **2006**, *313*, 80. (b) Ajayaghosh, A.; Varghese, R.; Goerge, S. J.; Vijayakumar, C. *Angew. Chem., Int. Ed.* **2006**, *45*, 1141. (c) Lohr, A.; Lysetska, M.; Würthner, F. *Angew. Chem., Int. Ed.* **2005**, *44*, 5071.

gregates according to the exciton chirality method,[13] which in the course of the fully reversible aggregation process transform upon increasing temperature into preferentially left-handed (*M*-configured) dimers. It is noteworthy that the magnitude of the observed CD intensities remains moderate in the investigated temperature range. Accordingly, despite the biased chemical equilibrium toward dimers with *M*-helicity and extended stacks with *P*-helicity, also their diastereomeric counterparts coexist in solution. However, upon decrease of temperature of PBI **3** solutions (Figure 2a,b), as well as for its thin films (Figure S3 in Supporting Information), the intensity of the CD signal increases, pointing to an increase of supramolecular order in the columnar π stacks of the bulk material that is further substantiated by dissymmetry factor g ($\Delta\epsilon/\epsilon$) values (Table S3 in Supporting Information).

The thermotropic behavior of **3** was studied by differential scanning calorimetry (DSC) and X-ray diffraction. The DSC measurements (Figure S4 in Supporting Information) revealed only one reversible phase transition from a LC phase into the isotropic liquid phase at 349 °C with an enthalpy change of $\Delta H = 28$ kJ mol^{-1} (19 J g^{-1}). The ΔH value of **3** is significantly larger than those observed for PBI derivatives **1** and **2** (9 and 19 kJ mol^{-1}, respectively),[6] implying a higher-ordered LC phase of **3**. This is also confirmed by a higher entropy change $\Delta S = 45$ J mol^{-1} K^{-1} for **3** for the isotropization process compared to **1** and **2** (14 and 33 J mol^{-1} K^{-1}, respectively). The higher order of the LC phase for **3** was further substantiated by the X-ray diffraction pattern (Figure S6, Table S4 in Supporting Information) of a powder-like sample that can be interpreted in terms of a columnar hexagonal ordered (Col$_{ho}$) mesophase with a cell parameter of 3 nm and a defined intracolumnar distance of 3.5 Å between the chromophore planes. In contrast, disordered columnar hexagonal mesophases were observed for **1** and **2**. The above-mentioned results of DSC and X-ray diffraction analyses of **3** confirm the presence of a highly ordered mesophase, which exists over a very broad temperature range from 0 °C to its clearing point at 349 °C.

The semiconducting properties of the π stacks of PBI **3** in this mesophase were investigated by using the pulse-radiolysis time-resolved microwave conductivity (PR-TRMC) technique.[14,15] For the Col$_{ho}$ LC phase of **3** at room temperature, we obtained an isotropic TRMC lower mobility limit of 0.010 cm^2 V^{-1} s^{-1}, which appeared to be constant over a broad temperature range from room temperature to at least 100 °C. Because this kind of material only transports charge carriers along the columnar structures, a one-dimensional TRMC lower mobility limit of 0.030 cm^2 V^{-1} s^{-1} can be deduced and a one-dimensional TRMC mobility of 0.087 cm^2 V^{-1} s^{-1} could be estimated (for details see Supporting Information). For comparison, we have also determined the one-dimensional TRMC lower mobility limit for the achiral PBI **2** in the Col$_{hd}$ phase (at 110 °C), which is amounted to only 0.0078 cm^2 V^{-1} s^{-1}. Hence, the TRMC mobility value for the LC state of **3** is about 4 times higher than that for the Col$_{hd}$ mesophase of PBI **2**. This can be explained in terms of higher intracolumnar order in the LC phase of **3**, which is an outcome of the helical arrangement imparted by the chiral side chains.

In conclusion, PBI dye **3** with appended chiral side chains has provided valuable insight into the stepwise growth of one-dimensional molecular aggregates in solution, and the impact of helical order on charge-carrier mobilities for a highly promising class of organic *n*-type semiconductors has been shown. Taken together, from the present observations and some other recent results from our and other laboratories,[12] we have learned that one should be cautious of drawing premature and far-reaching conclusions with regard to the uniformity of supramolecular species based on concentration- and temperature-dependent UV/vis spectra with well-defined isosbestic points.

Acknowledgment. Financial support by the Deutsche Forschungsgemeinschaft within the research training school GK 1221 is gratefully acknowledged.

Supporting Information Available: Synthesis and characterization of PBI **3** and additional spectroscopic and analytical data. This material is available free of charge via the Internet at http://pubs.acs.org.

OL0700963

---

[13] Berova, N.; Nakanishi, K.; Woody, R. W. *Circular Dichroism: Principles and Applications*; Wiley-VCH: New York, 2000.

[14] Warman, J. M.; de Haas, M. P.; Dicker, G.; Grozema, F. C.; Piris, J.; Debije, M. G. *Chem. Mater.* **2004**, *16*, 4600.

[15] PR-TRMC charge-carrier mobilities have been reported for crystalline, plastic crystalline, and liquid crystalline perylene bisimides: (a) Struijk, C. W.; Sieval, A. B.; Dakhorst, J. E. J.; van Dijk, M.; Kimkes, P.; Koehorst, R. B. M.; Donker, H.; Schaafsma, T. J.; Picken, S. J.; van de Craats, A. M.; Warman, J. M.; Zuilhof, H.; Sudholter, E. J. R. *J. Am. Chem. Soc*. **2000**, *122*, 11057. (b) Chen, Z.; Debije, M. G.; Debaerdemaeker, T.; Osswald, P.; Würthner, F. *ChemPhysChem.* **2004**, *5*, 137. (c) An, Z.; Yu, J.; Jones, S. C.; Barlow, S.; Yoo, S.; Domercq, B.; Prins, P.; Siebbeles, L. D. A.; Kippelen, B.; Marder, S. R. *Adv. Mater*. **2005**, *17*, 2580. (d) Debije, M. G.; Chen, Z.; Piris, J.; Neder, R. B.; Watson, M. M.; Müllen, K.; Würthner, F. *J. Mater. Chem.* **2005**, *15*, 1270.